# Supplementary Information

## Pore-Space-Partitioned Metal-Organic Frameworks for Sensitive and Selective Recognition of 2,4,6-Trinitrophenol

Meng-Le Tuo, Nan Song, Chen-Chen Xing, Quan-Guo Zhai*

*Key Laboratory of Applied Surface and Colloid Chemistry (MOE), School of Chemistry & Chemical Engineering, Shaanxi Normal University, Xi'an, Shaanxi, 710062, China,*

**Corresponding author, zhaiqg@snnu.edu.cn (Q.-G Zhai)*

# Contents

**X-ray single crystal structure determinations** ..... **2**

**Determination of detection limit** ..... **2**

**Ultraviolet absorption spectra** ..... **2**

**Solid-state and solvent-dependent luminescence** ..... **3**

**Fluorescence titration and recycling process** ..... **3**

**Experimental** ..... **4**

- **Table S1** ..... **4**
- **Figure S1** ..... **5**
- **Table S2** ..... **6**
- **Table S3** ..... **7**
- **Figure S2** ..... **7**
- **Figure S3** ..... **8**
- **Figure S4** ..... **8**
- **Figure S5** ..... **9**
- **Figure S6** ..... **10**
- **Figure S7** ..... **11**
- **Figure S8** ..... **12**
- **Figure S9** ..... **13**
- **Figure S10** ..... **14**
- **Figure S11** ..... **15**
- **Figure S12** ..... **16**
- **Figure S13** ..... **17**
- **Figure S14** ..... **18**
- **Figure S15** ..... **18**

**X-ray single crystal structure determinations**

Single-crystal X-ray analyses of SNNU-290 (CCDC: 2470144), SNNU-291 (CCDC: 2470145), SNNU-292 (CCDC: 2470146), and SNNU-293 (CCDC: 2470147) were all performed on a Bruker Smart APEX II CCD area diffractometer equipped with a nitrogen-flow temperature controller. The analyses used graphite-monochromated Mo $K_\alpha$ radiation ($\lambda$ = 0.71073 Å) and operated in the ω and φ scan mode. The SADABS program was used for the absorption correction. The crystal structure was solved by direct methods and refined on $F^2$ by full-matrix least-squares using SHELXTL and Olex2 program. The non-hydrogen atoms were refined anisotropic thermal parameters and positions of the hydrogen atoms attached to carbon and nitrogen atoms were fixed at their ideal positions. The disordered solvent molecules were removed by the Solvent Mask in Olex2.

**Determination of detection limit**

The detection limit (LOD) of MOFs for TNP was determined from the equation: $LOD = K \times \sigma/S$, where $K$ = 2 or 3 (we take 3 in this case); $\sigma$ is the standard deviation of the blank solution; $S$ is the slope of the calibration curve.

**Ultraviolet absorption spectra**

The synthesized MOF materials were ground into powders and dispersed in DMF solution. After 10 minutes of ultrasonic treatment, a uniformly dispersed suspension was formed with a concentration of 1 mg/3 mL. Seven nitro explosives were prepared as 1 mg/10 mL solutions for subsequent experiments. The ultraviolet absorption experiments were conducted in the range of 300-800 nm by adding 3 mL of suspension or solution to a quartz cuvette. The experimental results showed that, except for TNP, the remaining six nitro explosives exhibited almost no absorption peaks in this range, while the absorption peak of TNP was observed at approximately 400 nm. The absorption peak of SNNU-293 was also located near 400 nm, indicating similar absorption characteristics to TNP.

**Solid-state and solvent-dependent luminescence**

First, the solid-state fluorescence spectra of five MOFs and five ligands were measured at room temperature. Then, taking SNNU-293 as an example, the fluorescence properties of the MOF in different organic solvents were systematically studied. In this study, solvents such as N,N′-dimethylformamide (DMF), ethanol ($C_2H_5OH$), acetonitrile ($CH_3CN$), dichloromethane ($CH_2Cl_2$), N,N′-dimethylacetamide (DMA), dimethyl sulfoxide (DMSO), methanol ($CH_3OH$), 1,4-dioxane (1,4-DO), and acetone (ACE) were selected. 3 mg sample of SNNU-293 was dispersed in 3 mL of solvent and sonicated for 10 minutes to ensure thorough dispersion. The resulting 3 mL dispersion was then transferred to a quartz cuvette for photoluminescence experiments. The excitation wavelength was set at 370 nm, and the emission spectra were recorded in the range of 385-680 nm.

**Fluorescence titration and recycling process**

Taking the detection of SNNU-293 as an example, a detailed explanation is provided. First, SNNU-293 was fully dispersed in N,N'-dimethylformamide (DMF) to prepare a homogeneous suspension with a concentration of 1 mg/3 mL, and sonicated for about 10 minutes to ensure uniform dispersion. Next, different concentrations of nitro-aromatic explosives (NAEs) were added to quartz cuvettes containing 3 mL of the SNNU-293 DMF suspension, followed by fluorescence measurements. The sensitivity and selectivity of SNNU-293 were studied by recording the fluorescence intensity changes caused by varying concentrations of NAEs.

For recovery experiments, SNNU-293 was again dispersed in DMF to prepare a 1 mg/3 mL suspension and sonicated to ensure uniform dispersion. Then, 50 ppm of nitro-aromatic explosives was added, and the fluorescence intensity was recorded. After detection, the sample was recovered from the suspension by centrifugation, washed five times with fresh DMF to remove unreacted NAEs, and dried with nitrogen gas before preparing for the next cycle. Similar procedures were followed for the five-cycle experiments to assess the repeatability and stability of SNNU-293.

## Experimental

**Table S1.** Information on the reagents used in this study.

| Reagent Name | Abbreviation | Chemical Formula | Purity | Manufacturer |
|---|---|---|---|---|
| 2,5-Dihydroxyterephthalic acid | DHBDC | $C_8H_6O_6$ | 98% | Bide Pharmatech |
| Zinc nitrate hexahydrate | - | $Zn(NO_3)_2 \cdot 6H_2O$ | ≥99.5% | Sinopharm |
| 4-acetylpyridine | - | $C_7H_7NO$ | ≥98% | Bide Pharmatech |
| 4-pyridinecarboxaldehyde | - | $C_6H_5NO$ | 99.88% | Bide Pharmatech |
| 1,3,5-Tri(pyridin-4-yl)benzene | TPB | $C_{21}H_{15}N_3$ | ≥99.9% | Bide Pharmatech |
| 6-(Pyridin-4-yl)-4,2',4',4''-terpyridine | TPP | $C_{20}H_{14}N_4$ | ≥99.9% | Synthesized per literature |
| 2,4,6-Tri(4-pyridyl)-1,3,5-triazine | TPT | $C_{18}H_{12}N_6$ | ≥99.9% | Yan Zhong Tech |
| Tris(4-pyridyl)amine | TPA | $C_{15}H_{12}N_4$ | ≥99.9% | Yan Zhong Tech |
| Hexafluoroacetylacetone | HFP | $C_5H_2F_6O_2$ | ≥99.9% | TCI Chemicals |
| N,N-Dimethylformamide | DMF | $C_3H_7NO$ | AR | Sinopharm |
| N,N-Dimethylacetamide | DMA | $C_4H_9NO$ | AR | Sinopharm |
| 1,3-Dimethyl-3,4,5,6-tetrahydro-2(1H)-pyrimidinone | DMPU | $C_6H_{12}N_2O$ | 99% | Bide Pharmatech |
| Tetrafluoroboric acid | - | $HBF_4$ | >40% | Aladdint |
| Methanol | MeOH | $CH_3OH$ | AR | Sinopharm |
| Ethanol | EtOH | $C_2H_5OH$ | AR | Sinopharm |
| Acetonitrile | - | $CH_3CN$ | AR | Sinopharm |
| Dichloromethane | - | $CH_2Cl_2$ | AR | Sinopharm |
| Dimethyl sulfoxide | DMSO | $C_2H_6OS$ | AR | Sinopharm |
| Acetone | ACE | $C_3H_6O$ | AR | Sinopharm |
| Methanol | MeOH | $CH_3OH$ | AR | Sinopharm |

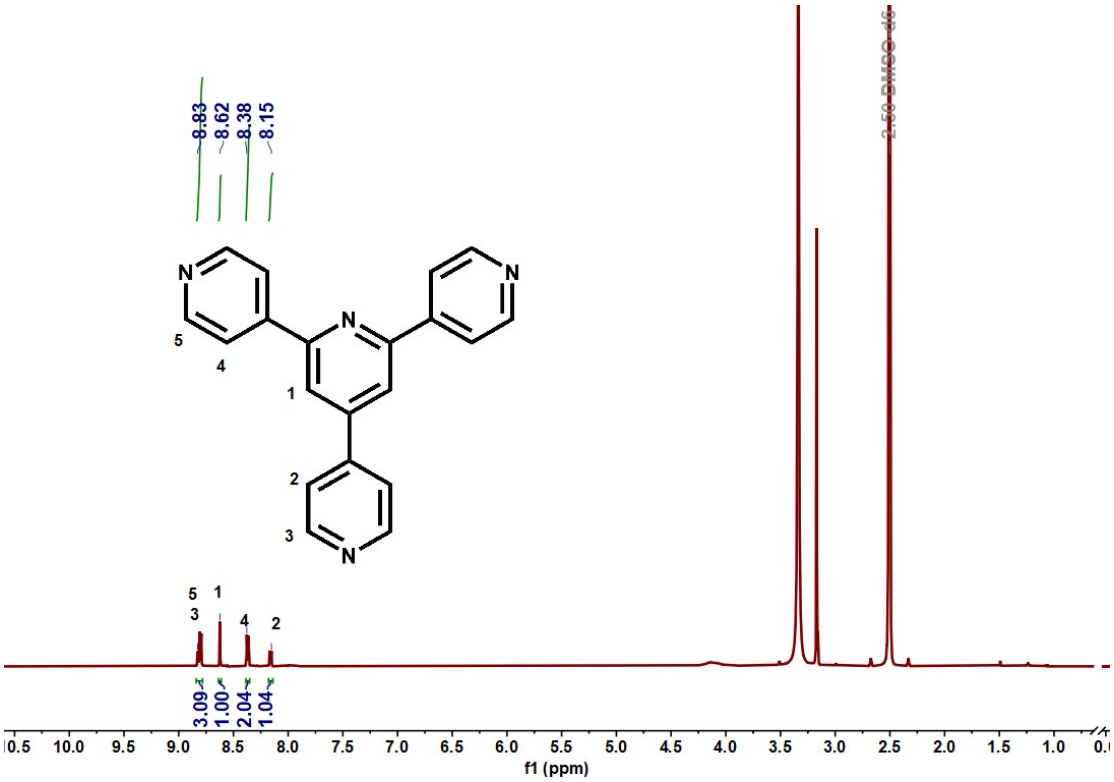


**Figure S1.** $^{1}$H NMR spectrum of TPP.

**Table S2.** Crystallographic data collection and structure refinements for SNNU-290-SNUU-293.

| Compounds | SNNU-290 | SNNU-291 | SNNU-292 | SNNU-293 |
|---|---|---|---|---|
| Empirical formula | $C_{45}H_{28}N_3O_{25}Zn_3$ | $C_{42}H_{28}N_6O_{28}Zn_3$ | $C_{42}H_{25}N_6O_{25}Zn_3$ | $C_{39}H_{25}N_4O_{19}Zn_3$ |
| Formula weight | 1206.81 | 1260.81 | 1260.81 | 1025.04 |
| Crystal system | Hexagonal | Hexagonal | Hexagonal | Hexagonal |
| space group | *P*63/*mmc* | *P*63/*mmc* | *P*63/*mmc* | *P*63/*mmc* |
| *a* (Å) | 17.16 | 17.06 | 16.92 | 14.53 |
| *b* (Å) | 17.16 | 17.06 | 16.92 | 14.53 |
| *c* (Å) | 15.27 | 15.33 | 15.41 | 17.80 |
| *α* (°) | 90 | 90 | 90 | 90 |
| *β* (°) | 90 | 90 | 90 | 90 |
| *γ* (°) | 120 | 120 | 120 | 120 |
| Volume ($Å^3$) | 3895.5(3) | 3867.8(3) | 3819.9(3) | 3258.2(4) |
| *Z* | 2 | 2 | 2 | 2 |
| Calculated density ($g/cm^3$) | 1.029 | 1.083 | 1.075 | 1.045 |
| *F* (000) | 1218.0 | 1272.0 | 1256.0 | 1009.0 |
| Limiting indices | -23 ≤ h ≤ 23, -23 ≤ k ≤ 24, -21 ≤ l ≤ 21 | -24 ≤ h ≤ 19, -15 ≤ k ≤ 24, -20 ≤ l ≤ 19 | -24 ≤ h ≤ 20, -23 ≤ k ≤ 23, -21 ≤ l ≤ 16 | -15 ≤ h ≤ 19, -20 ≤ k ≤ 20, -24 ≤ l ≤ 23 |
| Reflections /unique | 23121/2246 | 22498/2169 | 23587/2181 | 23435/3256 |
| *R*(int) | 0.0661 | 0.0532 | 0.0665 | 0.0495 |
| Data/restraints/parameter | 2246/0/76 | 2169/0/76 | 2181/0/75 | 3256/0/102 |
| Goodness-of-fit on $F^2$ | 1.086 | 1.126 | 1.123 | 0.974 |
| $R1^a$, $wR2^b$ [I>2δ (I)] | 0.0581, 0.1782 | 0.0646，0.2091 | 0.0702, 0.2434 | 0.0605, 0.2017 |
| $R1^a$, $wR2^b$ (all data) | 0.0674, 0.1836 | 0.0743，0.2174 | 0.0889, 0.2499 | 0.0810, 0.2137 |

$^a R1 = \Sigma||F_o|-|F_c|| / \Sigma|F_o|$. $^b wR_2 = [\Sigma w(F_o^2-F_c^2)^2 / \Sigma w(F_o^2)^2]$

**Table S3.** Pore structural parameters for SNNU-290-SNUU-293.

| | SNNU-290 | SNNU-291 | SNNU-292 | SNNU-293 |
|---|---|---|---|---|
| Cage1/ Å | ~4.4 | ~4.4 | ~4.4 | ~4.1 |
| Cage2/ Å | ~2.2 | ~2.3 | ~2.3 | ~2.6 |
| Cavity volumes/ Å$^3$ | 2123 | 2103 | 2017 | 1662 |
| Porosity | 52.0% | 52.8% | 54.4% | 54.5% |

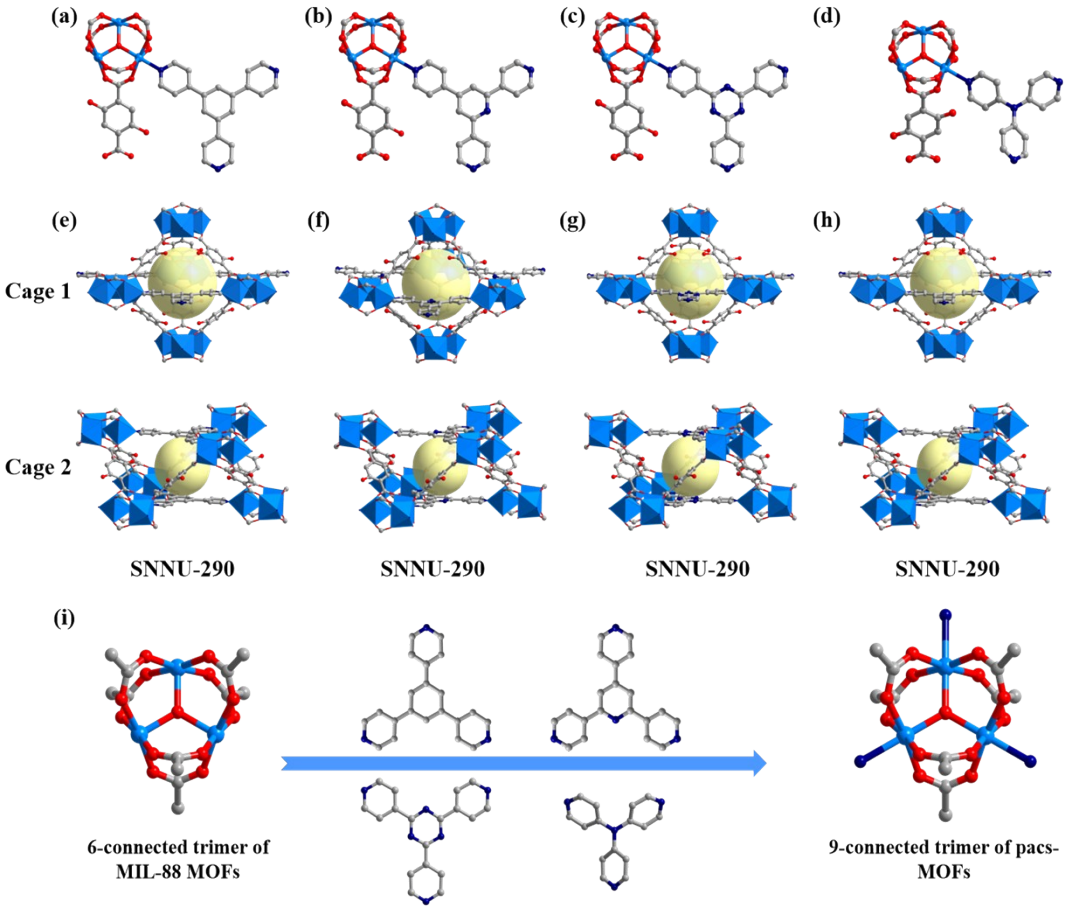


**Figure S2.** Coordination environments of compounds SNNU-290 (a), SNNU-291 (b), SNNU-292 (c) and SNNU-293 (d). Two cages in SNNU-290 (e), SNNU-291 (f), SNNU-292 (g) and SNNU-293 (h). (i) Schematic diagram of trinuclear cluster changes.

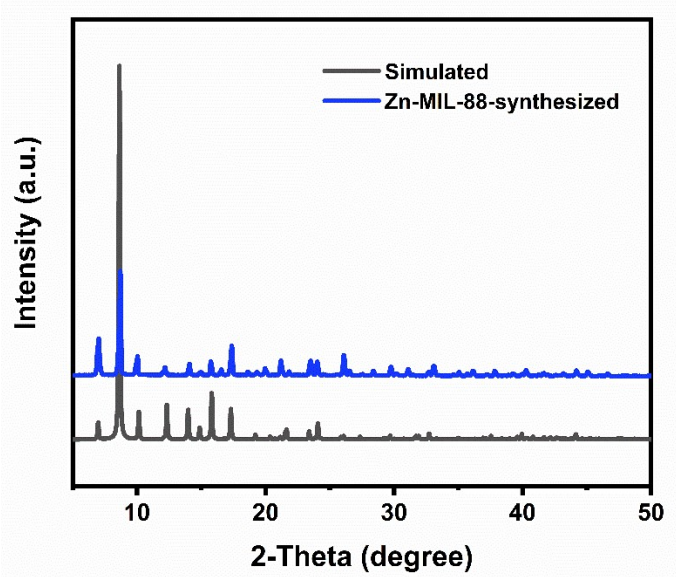


**Figure S3.** PXRD patterns for simulated and as-synthesized Zn-MIL-88.

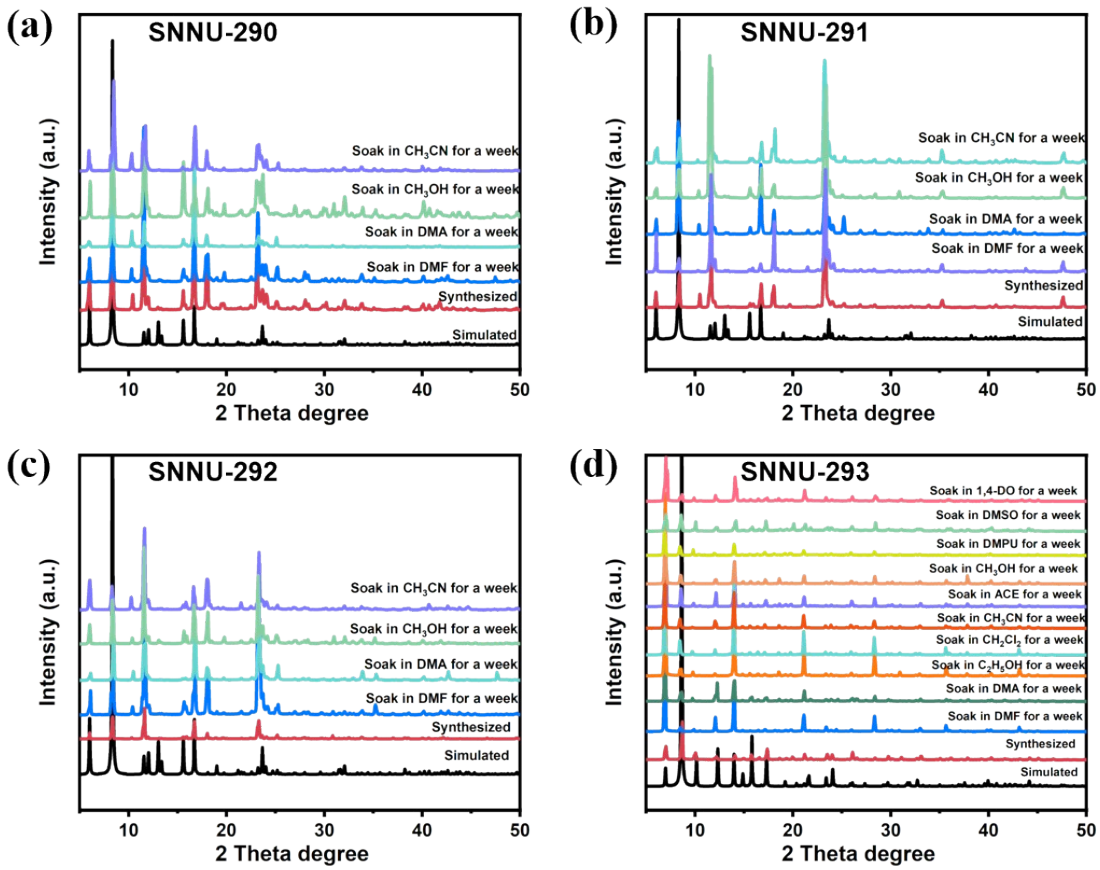


**Figure S4.** PXRD patterns of SNNU-290, SNNU-291, SNNU-292 and SNNU-293 after soaked in different solvents for a week.

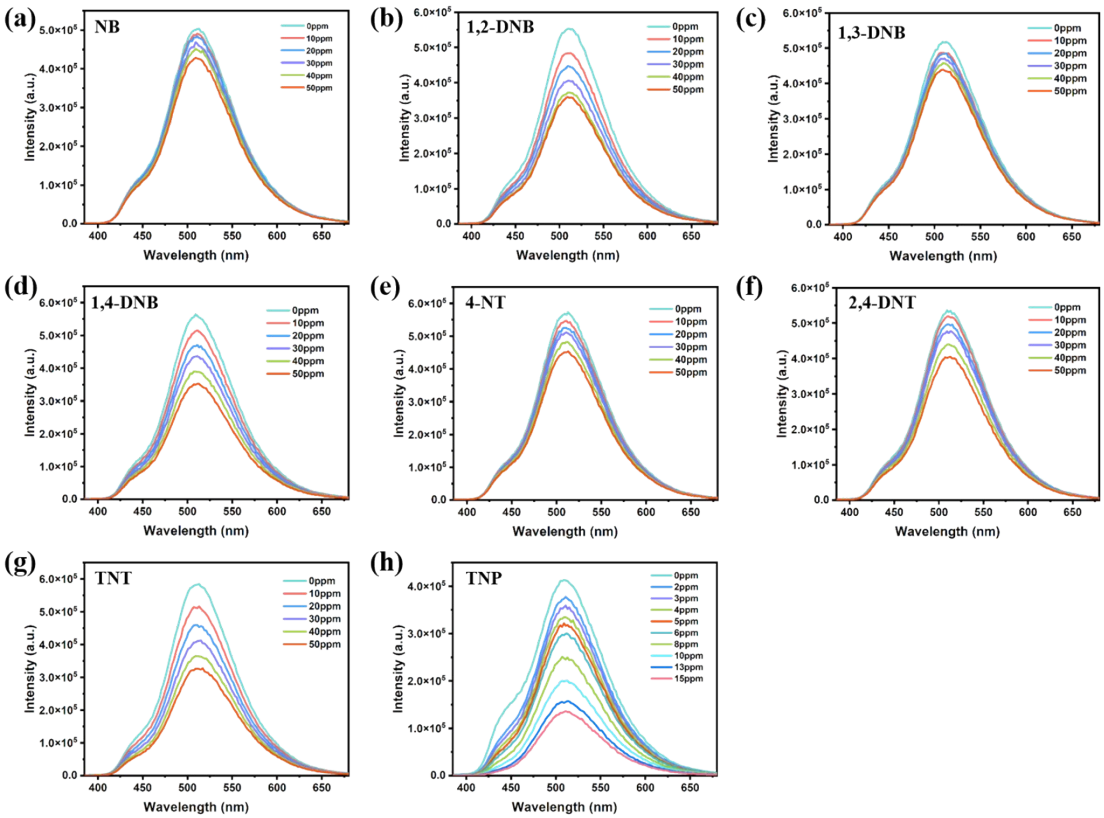


**Figure S5.** Fluorescence responses of Zn-MIL-88 in DMF solvent to different concentrations of NB (a), 1,2-DNB (b), 1,3-DNB (c), 1,4-DNB (d), 4-NT (e), 2,4-DNT (f), TNT (g), and TNP (h).

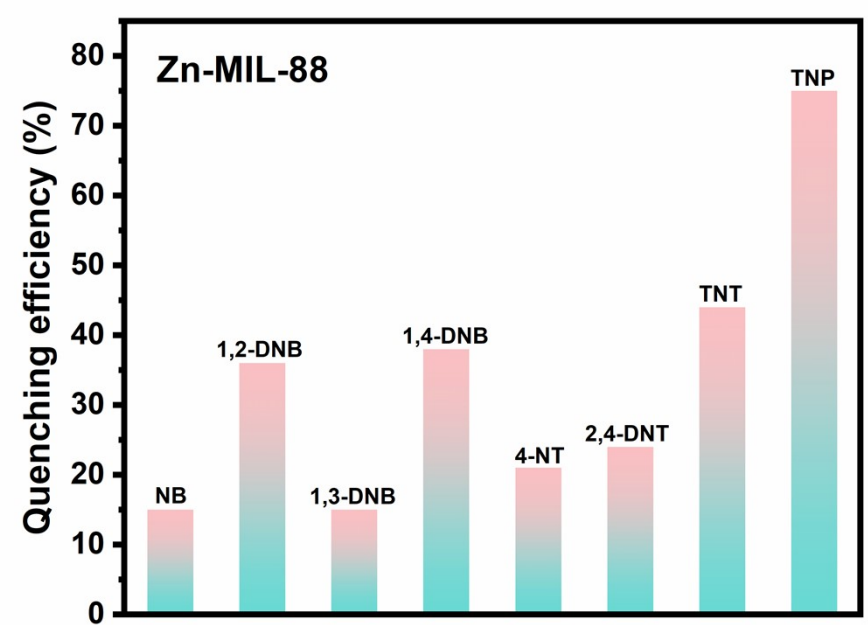


**Figure S6.** (a) The fluorescence quenching efficiency of Zn-MIL-88 after the addition of 50 ppm of different NAEs.

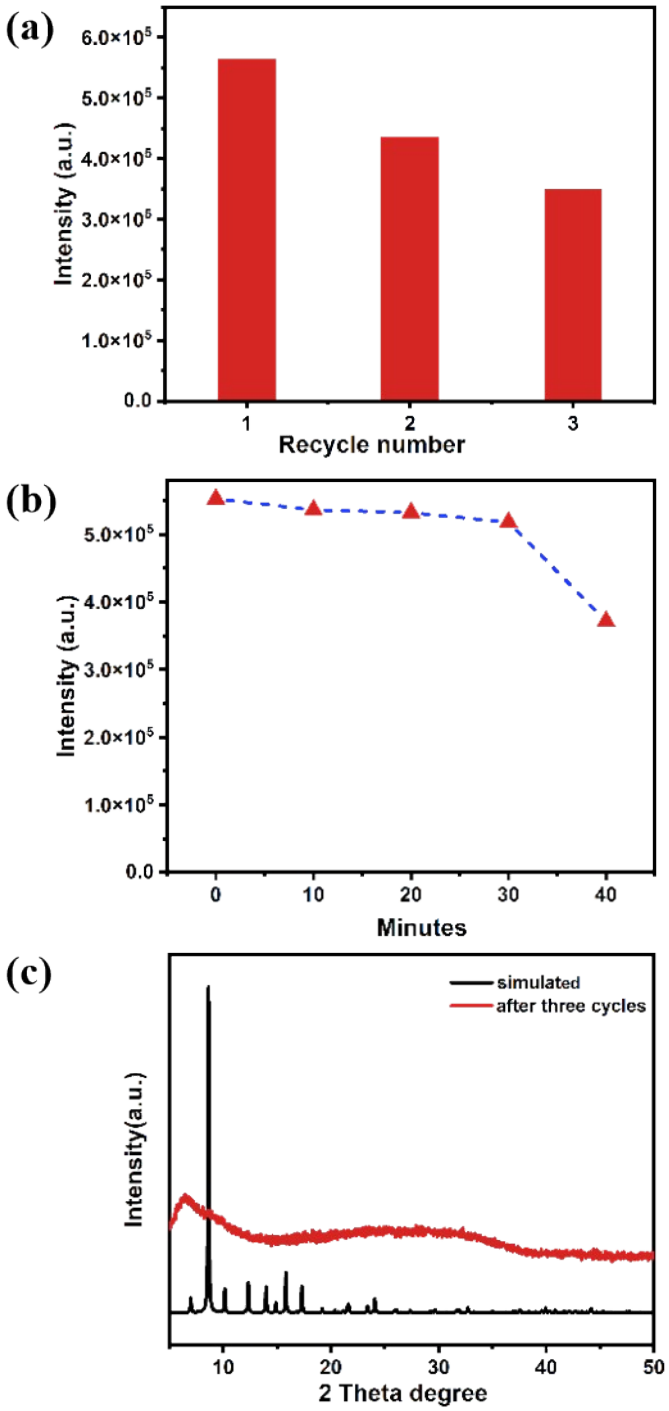


**Figure S7.** (a) The cycling stability of Zn-MIL-88. (b) Photostability of Zn-MIL-88.(c) PXRD patterns after three cycles.

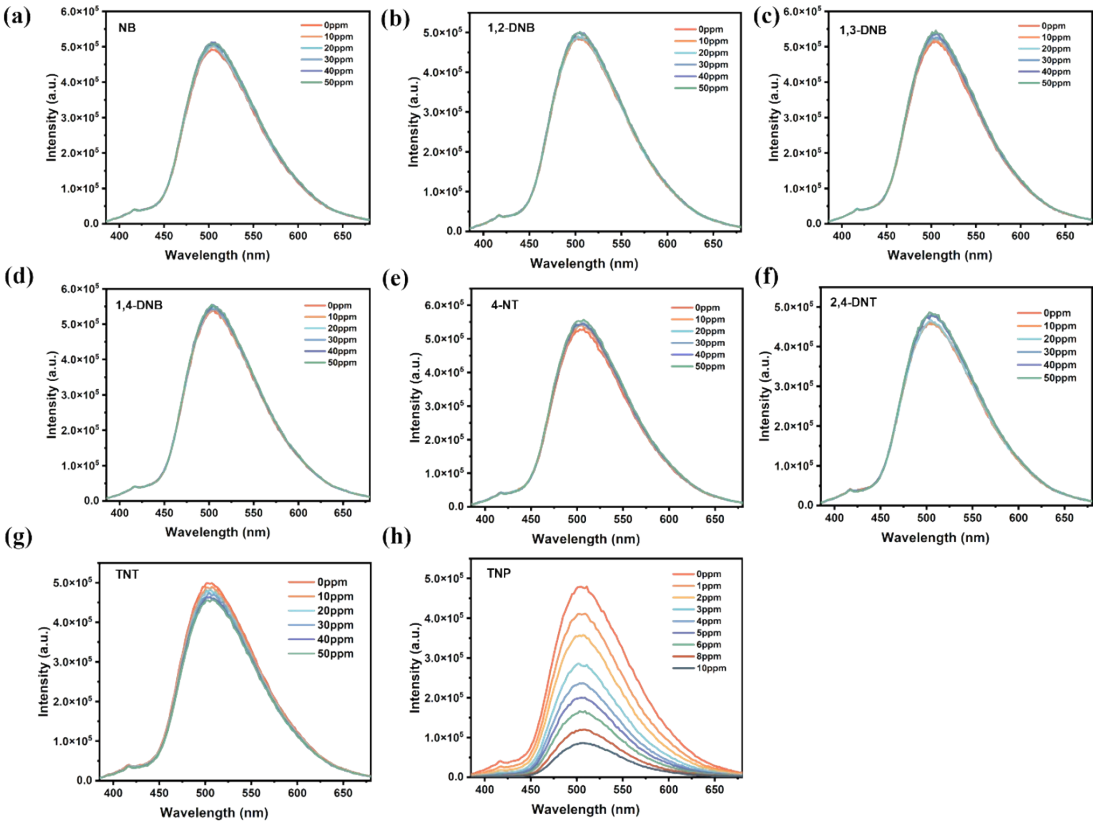


**Figure S8.** Fluorescence responses of SNNU-290 in DMF solvent to different concentrations of NB (a), 1,2-DNB (b), 1,3-DNB (c), 1,4-DNB (d), 4-NT (e), 2,4-DNT (f), TNT (g), and TNP (h).

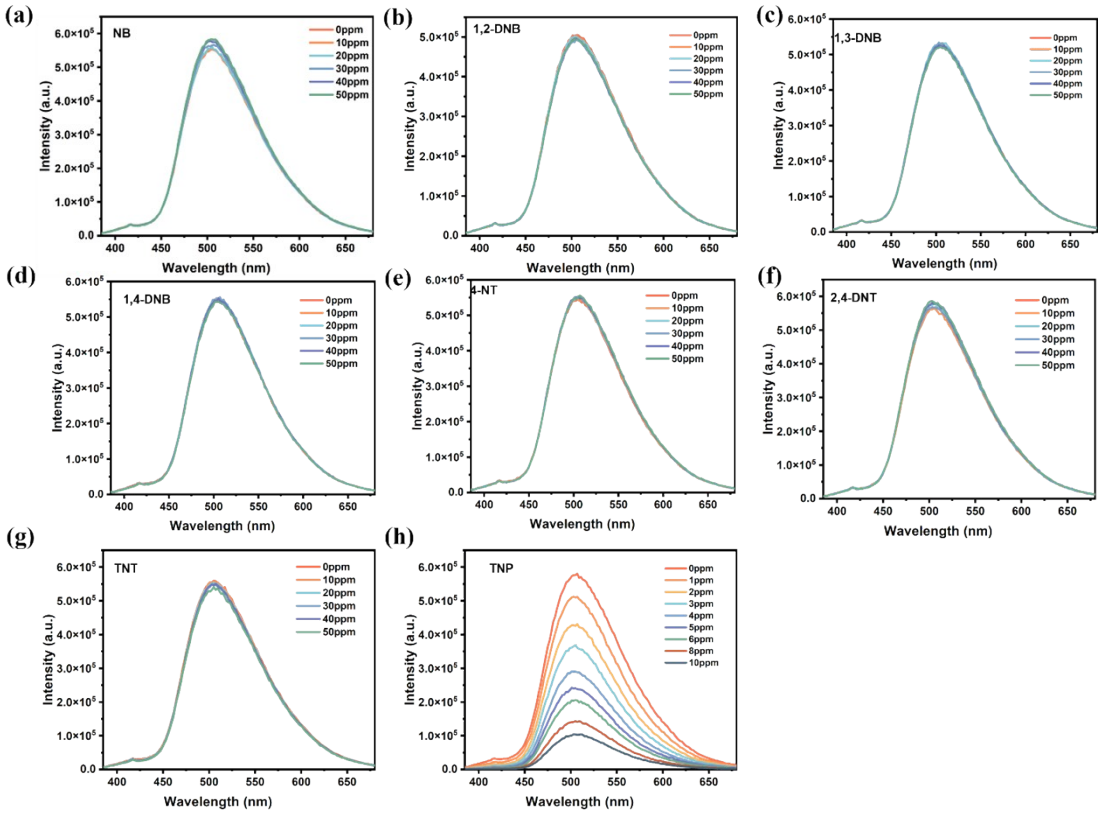


**Figure S9.** Fluorescence responses of SNNU-291 in DMF solvent to different concentrations of NB (a), 1,2-DNB (b), 1,3-DNB (c), 1,4-DNB (d), 4-NT (e), 2,4-DNT (f), TNT (g), and TNP (h).

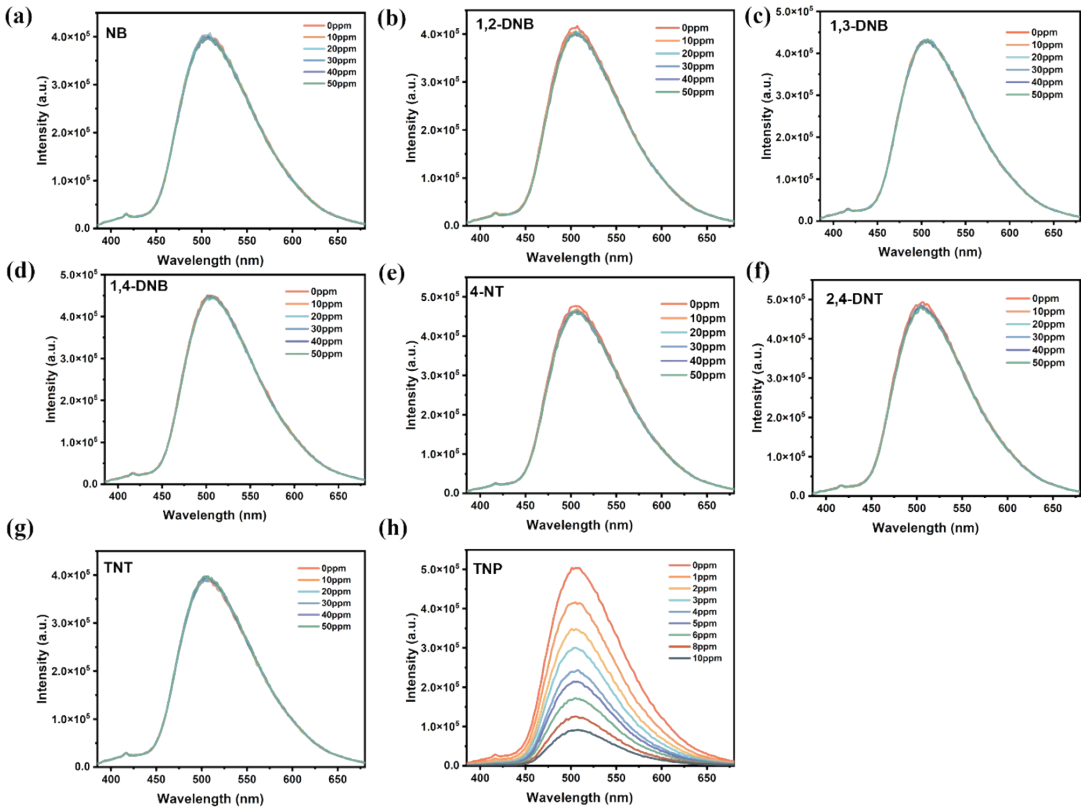


**Figure S10.** Fluorescence responses of SNNU-292 in DMF solvent to different concentrations of NB (a), 1,2-DNB (b), 1,3-DNB (c), 1,4-DNB (d), 4-NT (e), 2,4-DNT (f), TNT (g), and TNP (h).

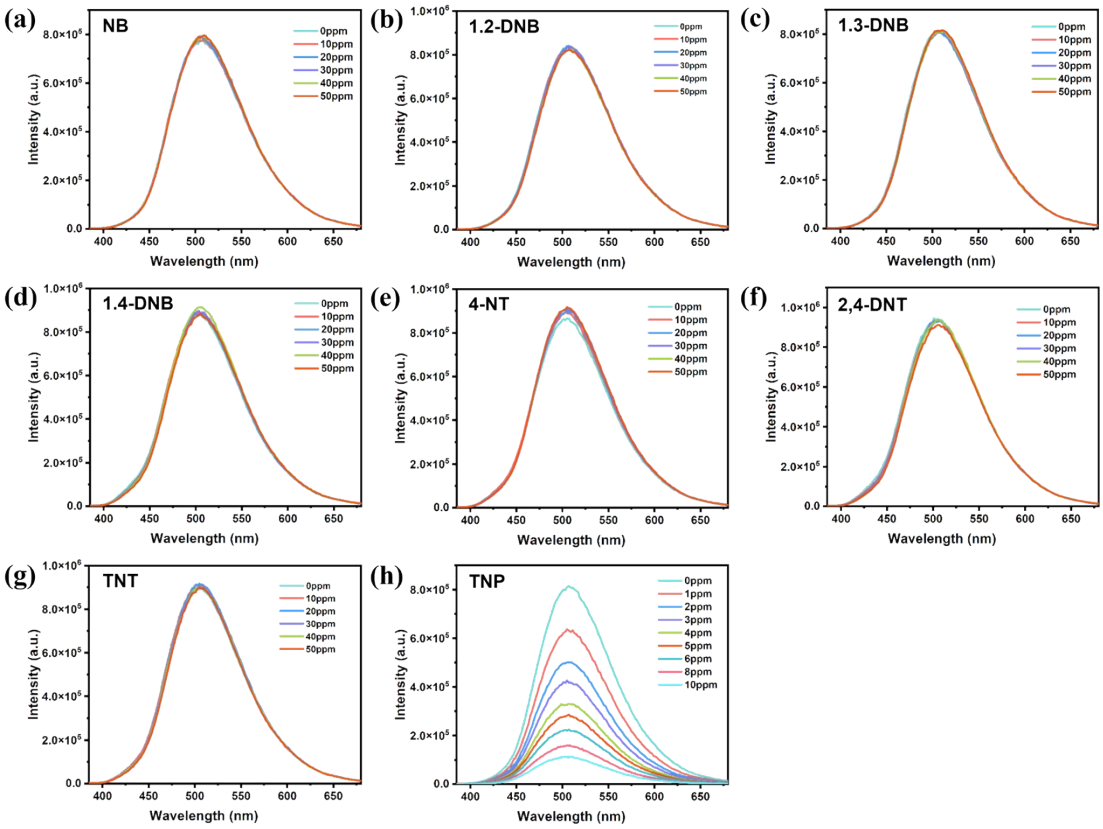


**Figure S11.** Fluorescence responses of SNNU-293 in DMF solvent to different concentrations of NB (a), 1,2-DNB (b), 1,3-DNB (c), 1,4-DNB (d), 4-NT (e), 2,4-DNT (f), TNT (g), and TNP (h).

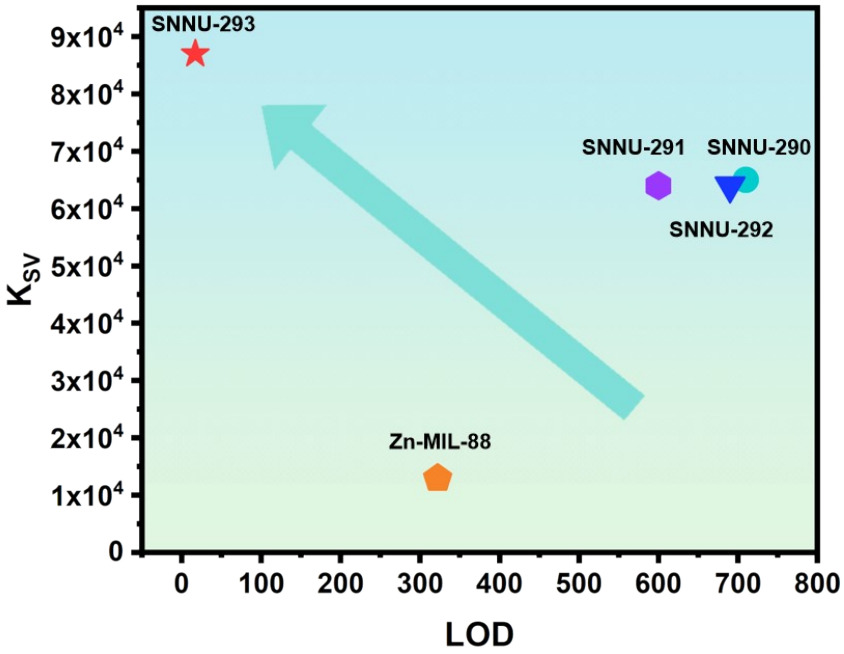


**Figure S12.** Summary of $K_{SV}$ and LOD values.

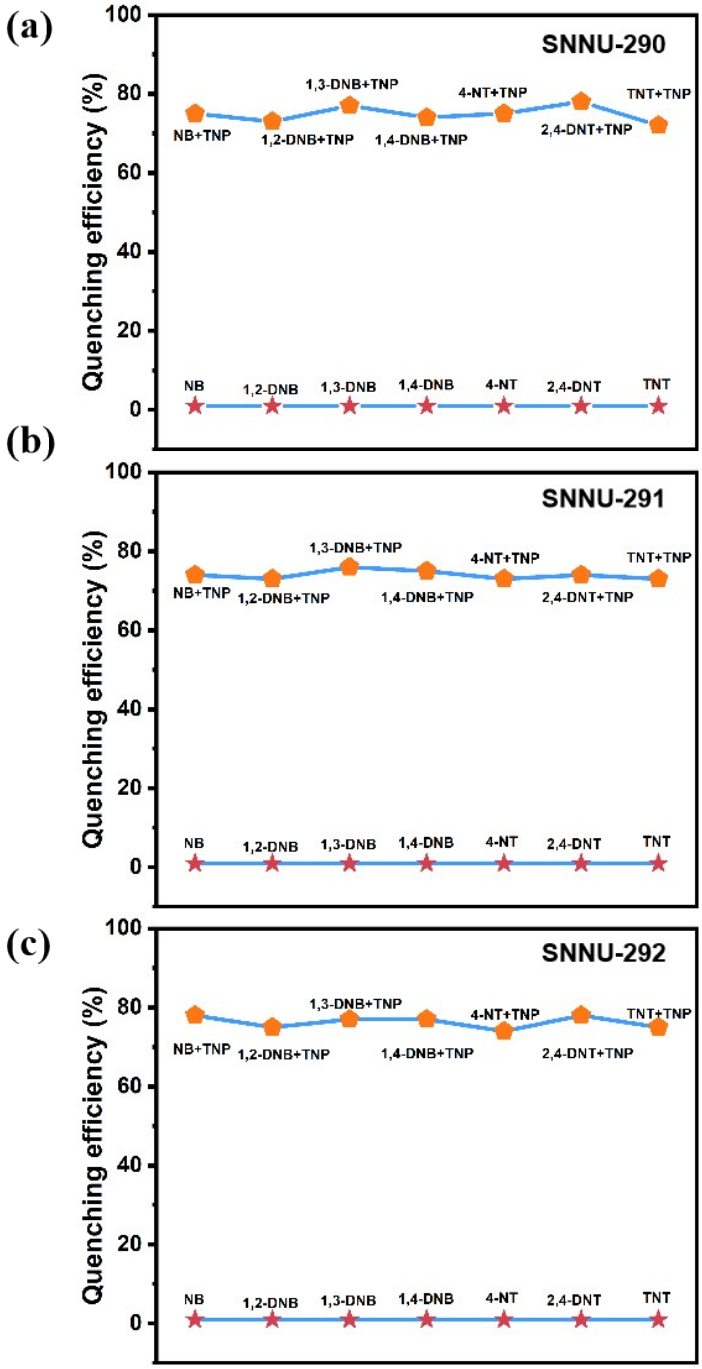


**Figure S13.** Photostability experimental data of SNNU-290 (a), SNNU-291 (b), SNNU-292 (c).

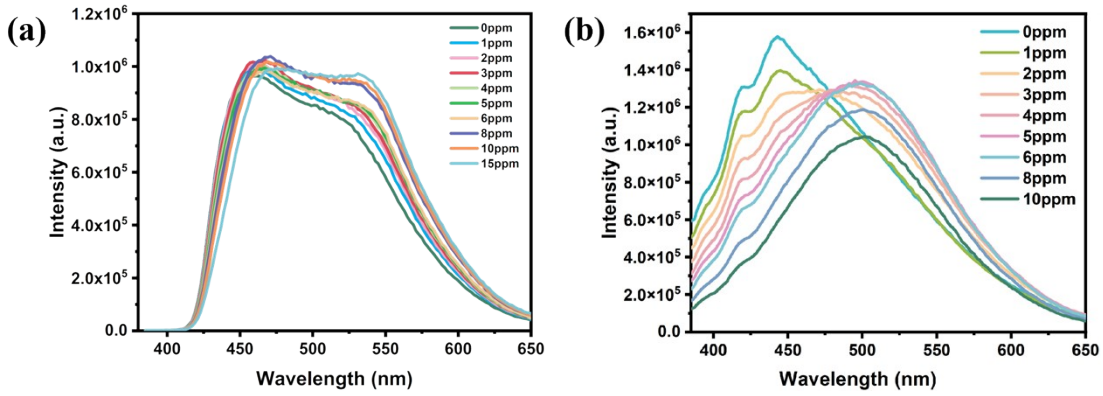


**Figure S14.** Sensing of TNP by DHBDC (a) and TPA (b).

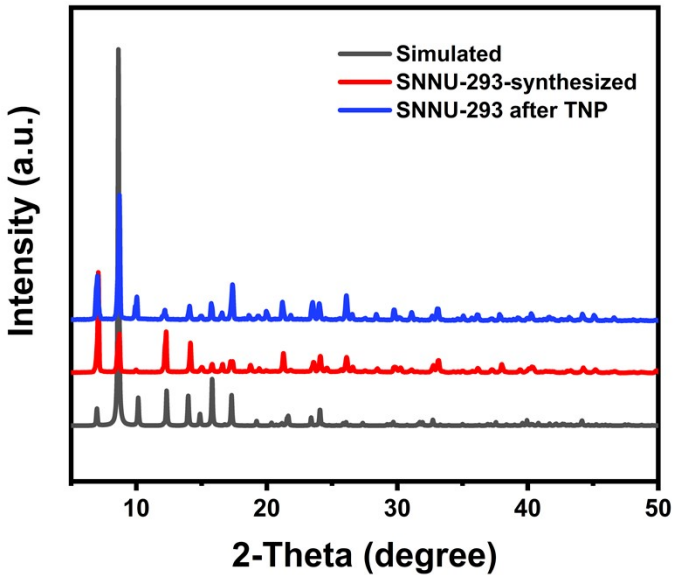


**Figure S15.** PXRD patterns of SNNU-293 before and after TNP sensing.